Far-field free tapping-mode tip-enhanced Raman microscopy

Jun Yu,[1] Yuika Saito,[1] Taro Ichimura,[2] Satoshi Kawata,[1,a)] and Prabhat Verma[1,b)]
[1]*Department of Applied Physics, Osaka University, Suita, Osaka 565-0871, Japan*
[2]*Quantitative Biology Center, RIKEN, Suita, Osaka 565-0874, Japan*

(Received 6 February 2013; accepted 20 March 2013; published online 28 March 2013)

A tip-enhanced Raman scattering (TERS) microscope has been developed, which is based on the tapping-mode operation of atomic force microscopy. By synchronizing a multichannel detector with tapping oscillation of the metallic nanotip, one can measure a tip-sample separation dependent TERS spectrum and dynamically obtain both near- and far-field Raman signals during the periodic oscillation of the tip. This facilitates TERS imaging with *in situ* point-by-point removal of far-field background, resulting in higher contrast in TERS imaging. Furthermore, we can obtain an extremely high spatial resolution of 8 nm. Also, tapping mode operation of tip has an added advantage of low sample damage, which could be important for future application of TERS to soft biological materials. Our TERS imaging technique enables us to construct far-field-free high-contrast near-field image at faster imaging speed with extremely high spatial resolution. [http://dx.doi.org/10.1063/1.4799496]

Tip-enhanced Raman scattering (TERS) has emerged over the past decade as a powerful tool for Raman spectroscopy that shows high sensitivity[1–6] and capability of nanoscale imaging with extremely high spatial resolution.[7–13] TERS utilizes a metallic nanotip, which, on a resonant excitation of localized surface plasmons, confines and enhances the propagating light into near-field in the close vicinity of the tip apex.[14–19] If a sample is brought near the tip apex within this confined light, TERS can be observed and Raman signal from the sample can be greatly enhanced. Further, by scanning the tip over the sample, for example, by means of an atomic force microscopy (AFM) control, one can obtain Raman image at extremely high spatial resolution.[7–9] Since the near-field light at the tip apex is excited by a propagating light, it is always accompanied with a far-field propagating light. Therefore, the near-field enhanced Raman signal in TERS is always accompanied with a far-field Raman signal originating from the scattering of the propagating light, which actually constitutes a far-field background in TERS measurement. Many reports on TERS microscopy have shown Raman images that include such far-field background.[20–22] However, this method is not suitable for weakly enhanced samples, because the enhanced signal can be buried in the far-field background, resulting in poor contrast or missing information in the image. Pure near-field Raman signal in TERS can only be obtained by subtracting this far-field background, which is usually done by measuring Raman spectrum twice—once by bringing a metallic nanotip close to the sample and once by retracting the tip away from the sample. The first spectrum would contain a combination of both near-field and far-field Raman signals, while the second spectrum would contain only the far-field Raman signal. Thus, one can obtain a pure near-field TERS spectrum by subtracting the second spectrum from the first one. A pure near-field Raman image in TERS microscopy can be similarly constructed by subtracting the Raman images obtained by keeping the tip retracted from the Raman image obtained by keeping the tip in contact with the sample.[23] In this method, while one can get pure near-field image, it is time consuming as well as there is a possibility of spatial shift between the two images, which can result in poor quality of the subtracted image. One possible way to overcome this problem could be to measure Raman signals at each scanning point of an image two times, by bringing the tip close to the sample and by retracting the tip away from the sample. By subtracting these two signals, one can get pure near-field Raman signal for that particular scanning point, before moving to the next scanning point. In this way, one can perform dynamic *in situ* far-field background removal for each scanning point individually during the imaging process, and obtain a pure near-field TERS image.

Since the confinement of light near tip apex in TERS originates from the oscillation of localized surface plasmons, it decays quickly as one moves away from the tip apex, causing the enhancement in Raman scattering to decrease with increasing tip-sample separation. Thus, the enhancement of Raman signal in TERS strongly depends on the tip-sample separation. Some of the present authors studied this phenomenon in the past by controlling the tip through the tapping mode operation of AFM, instead of the conventional contact mode operation, which was synchronized with a dual-gated photon counting system.[24] The tip oscillates perpendicular to the sample surface in tapping-mode operation, which effectively changes the tip-sample separation sinusoidally. By measuring the TERS signal at different tip-sample separation during the tip oscillation, the authors investigated the confinement of enhanced field near the tip apex. It was found that light field was strongly confined to the tip apex within a few nanometers, and it decayed to negligible intensity for the largest tip-sample separation. This means, it is possible to measure both Raman signals, one when tip is in contact with sample and another when the tip is retracted from the sample, during the oscillation of the tip.

By following this idea of dynamically measuring Raman signals at minimum and maximum tip-sample separations using the tapping mode operation of AFM, in this letter, we

[a)]Also at RIKEN, Wako, Saitama 351-0198, Japan.
[b)]Electronic mail: verma@ap.eng.osaka-u.ac.jp

have extended our previous work to obtain pure near-field TERS images. Here, we employ a synchronized multichannel detector and demonstrate TERS microscopy for *in situ* removal of far-field background and show some TERS images obtained for single walled carbon nanotubes (SWNTs). We have also shown high spatial resolution as high as 8 nm in our imaging technique and found better image contrast compared to the conventional TERS microscopy using the contact mode operation of AFM.

As mentioned before, the conventional TERS microscopy utilizes contact-mode AFM for positioning and scanning the metallic tip on the sample surface.[25] Some researchers also use the scanning tunneling microscopy techniques for manipulating the tip position. While the first technique maintains the tip in contact with the sample, the other keeps the tip at a fixed small separation needed for the feedback of tunneling current. Apart from this, shear-force microscopy is also utilized, where the tip oscillates parallel to the sample surface and a small but constant tip-sample separation is maintained.[26,27] Since it is possible to choose a tip-sample separation in shear-force configuration, this technique can also be potentially utilized for tip-sample separation depended TERS measurements. However, the accuracy of tip position in z-direction (along the tip axis) is very poor in shear-force technique, and the movement of the tip in z-direction is not as smooth. On the other hand, unlike the shear force microscopes, tapping mode AFM configuration[28,29] oscillates the tip in z-direction and may provide extremely high accuracy of about 0.3 nm of tip position in z-direction. Some researchers have utilized the tapping mode AFM for tip-sample separation dependent fluorescence measurements.[30,31] Thus, this technique can be utilized for high accuracy tip-sample separation dependent TERS measurement.

In our present measurement system, we utilized a multichannel detector, which has 64 detector channels. This detector is synchronized with the tapping oscillation of the AFM system in such a way that one tapping cycle is divided into 64 channels, which sequentially measure Raman intensity during the entire cycle. Therefore, each tapping cycle is divided into 64 measurements, corresponding to 64 different values of tip-sample separations during the tip oscillation. In other words, entire period of tip oscillation, which is about 8 μs in our experiments, is divided into 64 time-gates each with the width of 0.125 μs, and the 64 channels of the detector sequentially measure Raman intensity corresponding to each time-gate. Thus, if we open only one channel in the detector, we can measure Raman intensity corresponding to a specific tip-sample separation associated with that channel for as long acquisition time as needed. Similarly, if channel#1 and channel#32 correspond to the minimum and maximum tip-sample separations, respectively, then by opening these two channels in the detection system, we can measure Raman intensities corresponding to the minimum and the maximum tip-sample separations simultaneously. By subtracting these two Raman intensities, one can obtain *in situ* far-field-free pure near-field Raman signal from the sample. Then, by scanning the tip on the sample, one can obtain a far-field-free TERS image of the sample.

The experimental system utilized in the present study, which was based on an inverted optical microscope integrated with a tapping-mode AFM, can be understood from Fig. 1. The SWNT sample was spin casted on a glass substrate, which was placed on a piezo-controlled sample stage for scanning purpose. Raman scattering from SWNT was excited with a laser of wavelength 488 nm, which was tightly focused on the sample by a high-NA oil-immersion objective (NA = 1.4). The power density of illumination at the sample was 2.5×10^3 kW/cm^2. In order to produce evanescent illumination at the sample, the low-NA component (NA < 1) of the incident light was rejected by introducing a mask on the illumination path, as shown in Fig. 1(a).[32] The scattered light was collected by the same objective, which was measured through a spectrometer and an avalanche photodiode (APD). The Rayleigh scattered light was blocked by an edge filter. Raman spectrum measured from SWNTs shows strongest Raman peak at 1595 cm^{-1}, which corresponds to the G-mode vibrations. The spectrometer was set for the APD to detect Raman signal corresponding to this mode with a spectral window of 22 cm^{-1}. The output of the APD was sent to a multichannel photon counter (NanoHarp 250, PicoQuant), which was synchronized with the trigger signal supplied for tapping oscillation of AFM, as shown in Fig. 1(a). The metallic tip utilized in this study was prepared by evaporating thin layer of silver on a commercially available AFM cantilever tip made of silicon. The functioning of the multichannel photon counter can be understood from the illustration in Fig. 1(b). The upper curve shows the sinusoidal variation of the tip-sample separation D(t) as a function of time, and the middle illustration shows sequential 64 time-gates (with width Δt) synchronized with one tapping period. Since the tapping period in our experiment is 8 μs, the value of gate width, Δt, is 0.125 μs. The maximum and the minimum tip-sample separations, D_{max} and D_{min}, can be obtained at the peak and the valley positions of the sinusoidal curve, respectively. Since the tip taps on the sample surface during its oscillation, $D_{min} = 0$. The vertical dotted lines in Fig. 1(b) show that different time-gates correspond to different tip-sample separations. By opening a particular time-gate, one can repeatedly collect the Raman signal for the corresponding tip-sample separation. Similarly, by opening all the time-gates sequentially one after another, one can get tip-sample separation dependent Raman signal for the entire tapping oscillation period. This signal is expected to be maximum for $D(t) = 0$ and minimum for $D(t) = D_{max}$. The

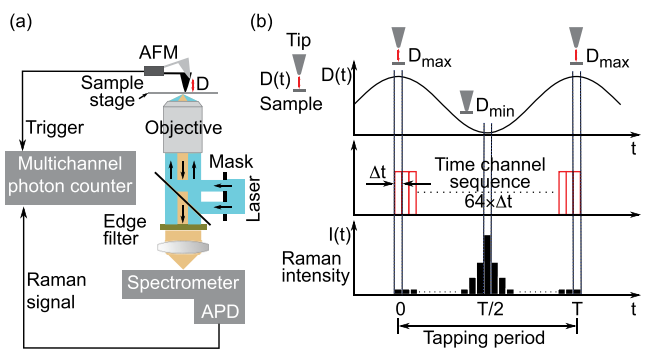

FIG. 1. (a) Experimental setup for tip-enhanced near-field Raman microscopy through tapping-mode AFM configuration. (b) Schematic of time-correlated photon counting for Raman measurement.

illustration in lower graph in Fig. 1(b) shows Raman intensities measured through corresponding time-gates in the middle illustration at the corresponding tip-sample separations depicted from the upper graph.

Before going for the *in situ* far-field background-free TERS imaging, we first employed our tapping-mode based TERS measurement system to evaluate the tip-sample separation dependent enhancement of Raman signal, as explained above. Figure 2(a) shows Raman intensity of the G-mode ($1595\,cm^{-1}$) of SWNT measured through the 64 time-gates during one tapping period, which was accumulated for 1 s. From the maximum value of the measured Raman intensity, we define point A in Fig. 2(a) as the time-gate where tip was in contact with the sample. Point B, which is half time period away from A, is defined as the time-gate where the tip-sample separation was maximum. The highest position of tip during its tapping oscillation was estimated through the force curve measurement,[24,33] which was found to be 113 nm in the present experiment. The time positions from points A to B in Fig. 2(a) correspond to the tip-sample separation of 0 to 113 nm during the tip oscillation. By dividing this tip-sample separation into 64 parts by keeping its sinusoidal nature into consideration, one can obtain a relation between the location of time-gate and the position of the tip. Thus, time-correlated Raman intensity can be converted into tip-sample separation dependent Raman intensity. After such conversion, Fig. 2(b) shows the tip-sample separation dependence of Raman intensity between points A and B from Fig. 1(a). As expected, Fig. 2(b) shows strong dependence of tip-sample separation on the enhancement of Raman signal. Raman intensity rapidly increases as the tip-sample separation decreases. The maximum enhancement factor at minimum tip-sample separation was estimated to be 1487, which was calculated by taking intensities and sample volumes into account. Further, one can see a constant background of 46 counts, indicated by the dotted line in Fig. 2(b), which is the far-field background independent of the tip-sample separation. The background count of the APD was about 1.25 counts/channel, which confirms that the measured background of 46 counts was much larger than the detector background.

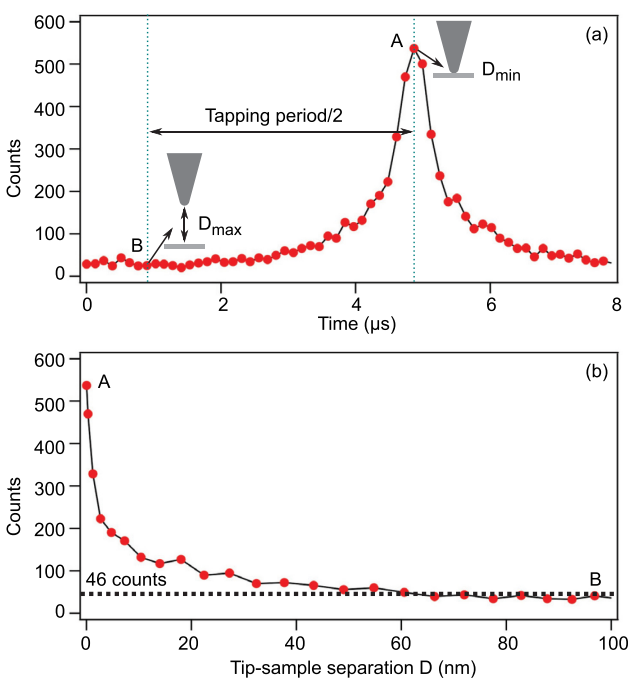

FIG. 2. (a) Time-correlated Raman intensity measured from the G-mode of SWNTs with our tapping-mode TERS system. (b) Tip-sample separation dependent Raman intensity converted from position A to position B in (a).

Raman intensity in Fig. 2(b) becomes almost constant for tip-sample separation larger than about 50 nm, indicating that when the tip is more than 50 nm away from the sample, Raman signal contains only far-field background. It is clear that by subtracting this background signal from Raman intensity at any chosen tip-sample separation, we can obtain pure near-field Raman signal at that particular value of the tip-sample separation. We performed this *in situ* far-field removal at D_{min} and raster scanned the sample at a step of 5 nm to obtain a far-field background free TERS image. Figure 3(a) shows a far-field free Raman image of SWNTs measured at the minimum tip-sample separation. At each scanning point, tip-sample separation dependent Raman intensity was measured and the pure near-field signal was obtained *in situ* by subtraction of far-field background signal at that point. For comparison, a conventional TERS image was measured by contact mode operation of AFM control where the tip was always in contact with the sample. This TERS image, which includes far-field background, is shown in Fig. 3(b). As it can be seen from Fig. 3, the far-field free TERS image obtained from our tapping mode system has much better contrast than the conventional TERS image, showing the advantage of our technique compared to the conventional method. We could also obtain high spatial resolution of 12 nm, which is estimated from the full width at half maximum (FWHM) of the line profile of Raman intensity along the dashed line in Fig. 3(a). Even though the spatial resolution of 12 nm is reasonably high in comparison to some existing work,[7–9] it is only slightly larger than twice the value of scanning step, which was 5 nm. In order to check the real strength of our technique in terms of spatial resolution, we imaged a small area of the sample with a reduced scanning step of 3 nm. The far-field free TERS image obtained with our tapping mode system with this shorter scanning step is shown in Fig. 4(a). Figure 4(b) shows a simultaneously obtained AFM image for comparison. Since this AFM image is obtained with the silver-coated tip used in TERS, the AFM image has poor quality; however, it

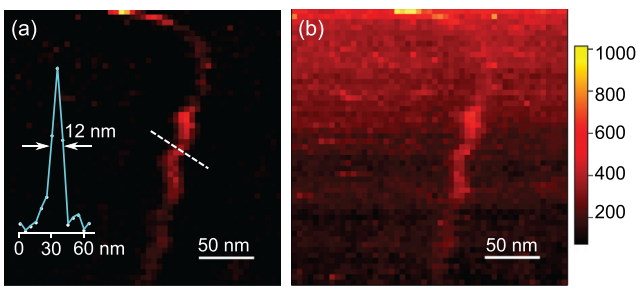

FIG. 3. (a) Far-field-free TERS image of SWNTs obtained from tapping mode system. The inset shows a line profile of Raman intensity along the dashed line. (b) Conventional TERS image obtained from a contact mode configuration that included far-field background signal. Both images have 50×50 pixels with pixel size of 5 nm, the acquisition time for each pixel is 1 s. The total measurement time was about 42 min.

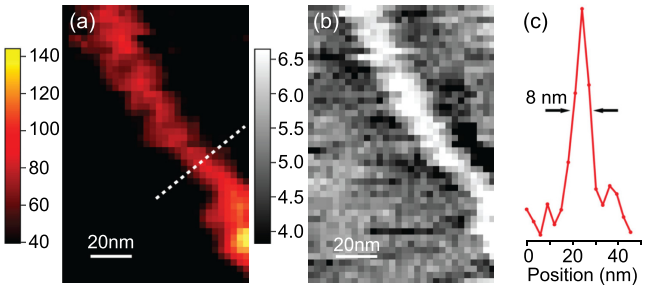

FIG. 4. (a) Far-field-free TERS image of SWNTs obtained from tapping mode system at a scanning step of 3 nm. Here, the image size is 30×45 pixels measured with the acquisition time of 0.5 s. The total measurement time is about 11 min. (b) Simultaneously obtained AFM image. (c) A line profile of Raman intensity along the dashed line shown in (a).

confirms the presence of SWNT sample with an average height of 2.8 nm, indicating that the sample was a bundle of 2–3 nanotubes. Figure 4(c) shows the line profile of Raman intensity measured along the dashed line in Fig. 4(a). The FWHM of this line profile shows that spatial resolution in far-field free TERS image is as high as 8 nm, which is an extremely high value.

In conclusion, we have developed a tapping-mode TERS microscope that can measure tip-sample separation dependent TERS signal via a synchronously time-gated multichannel detector. By dynamically measuring both near- and far-field Raman signals during the tapping period of tip oscillation, one can obtain pure near-field Raman image by *in situ* removal of far-field background. One of the additional advantages of this technique is that by using tapping-mode operation of AFM, we can avoid sample damage that a tip in contact mode can cause.[25,29] This could be important for future application of TERS to soft biological materials where the tip force applied on the sample may cause critical deformations. Furthermore, we can have a better image contrast and extremely high spatial resolution of 8 nm in our TERS imaging technique.

This work was supported by the Asian CORE Program of Japan Society for the Promotion of Science (JSPS).

[1]N. Hayazawa, T. Yano, H. Watanabe, Y. Inouye, and S. Kawata, Chem. Phys. Lett. **376**, 174 (2003).
[2]B. Pettinger, B. Ren, G. Picardi, R. Schuster, and G. Ertl, Phys. Rev. Lett. **92**, 096101 (2004).
[3]J. Stadler, T. Schmid, and R. Zenobi, Nano Lett. **10**, 4514 (2010).
[4]T. Deckert-Gaudig, E. Rauls, and V. Deckert, J. Phys. Chem. C **114**, 7412 (2010).
[5]C. Georgi and A. Hartschuh, Appl. Phys. Lett. **97**, 143117 (2010).
[6]N. Jiang, E. T. Foley, J. M. Klingsporn, M. D. Sonntag, N. A. Valley, J. A. Dieringer, T. Seideman, G. C. Schatz, M. C. Hersam, and R. P. Van Duyne, Nano Lett. **12**, 5061 (2012).
[7]A. Hartschuh, E. J. Sánchez, X. S. Xie, and L. Novotny, Phys. Rev. Lett. **90**, 095503 (2003).
[8]T. Ichimura, N. Hayazawa, M. Hashimoto, Y. Inouye, and S. Kawata, Phys. Rev. Lett. **92**, 220801 (2004).
[9]J. Steidtner and B. Pettinger, Phys. Rev. Lett. **100**, 236101 (2008).
[10]T. Ichimura, S. Fujii, P. Verma, T. Yano, Y. Inouye, and S. Kawata, Phys. Rev. Lett. **102**, 186101 (2009).
[11]T. Yano, P. Verma, Y. Saito, T. Ichimura, and S. Kawata, Nat. Photonics **3**, 473 (2009).
[12]P. Verma, T. Ichimura, T. Yano, Y. Saito, and S. Kawata, Laser & Photon. Rev. **4**, 548 (2010).
[13]B. Pettinger, P. Schambach, C. J. Villagómez, and N. Scott, Annu. Rev. Phys. Chem. **63**, 379 (2012).
[14]N. Hayazawa, Y. Inouye, Z. Sekkat, and S. Kawata, Opt. Commun. **183**, 333 (2000).
[15]M. S. Anderson, Appl. Phys. Lett. **76**, 3130 (2000).
[16]R. M. Stöckle, Y. D. Suh, V. Deckert, and R. Zenobi, Chem. Phys. Lett. **318**, 131 (2000).
[17]B. Hecht, H. Bielefeldt, L. Novotny, Y. Inouye, and D. W. Pohl, Phys. Rev. Lett. **77**, 1889 (1996).
[18]E. Hutter and J. H. Fendler, Adv. Mater. **16**, 1685 (2004).
[19]C. Noguez, J. Phys. Chem. C **111**, 3806 (2007).
[20]A. Hartschuh, N. Anderson, and L. Novotny, J. Microsc. **210**, 234 (2003).
[21]L. G. Cançado, A. Hartschuh, and L. Novotny, J. Raman Spectrosc. **40**, 1420 (2009).
[22]E. Bailo and V. Deckert, Chem. Soc. Rev. **37**, 921 (2008).
[23]T. Yano, P. Verma, S. Kawata, and Y. Inouye, Appl. Phys. Lett. **88**, 093125 (2006).
[24]T. Yano, T. Ichimura, A. Taguchi, N. Hayazawa, P. Verma, Y. Inouye, and S. Kawata, Appl. Phys. Lett. **91**, 121101 (2007).
[25]I. Schmitz, M. Schreiner, G. Friedbacher, and M. Grasserbauer, Anal. Chem. **69**, 1012 (1997).
[26]E. Betzig, P. L. Finn, and J. S. Weiner, Appl. Phys. Lett. **60**, 2484 (1992).
[27]W. A. Atia and C. C. Davis, Appl. Phys. Lett. **70**, 405 (1997).
[28]Q. Zhong, D. Inniss, K. Kjoller, and V. B. Elings, Surf. Sci. Lett. **290**, L688 (1993).
[29]P. K. Hansma, J. P. Cleveland, M. Radmacher, D. A. Walters, P. E. Hillner, M. Bezanilla, M. Fritz, D. Vie, H. G. Hansma, C. B. Prater, J. Massie, L. Fukunaga, J. Gurley, and V. Elings, Appl. Phys. Lett. **64**, 1738 (1994).
[30]E. Yoskovitz, G. Menagen, A. Sitt, E. Lachman, and U. Banin, Nano Lett. **10**, 3068 (2010).
[31]B. D. Mangum, C. Mu, and J. M. Gerton, Opt. Express **16**, 6183 (2008).
[32]N. Hayazawa, Y. Inouye, and S. Kawata, J. Microsc. **194**, 472 (1999).
[33]C. Su, L. Huang, and K. Kjoller, Ultramicroscopy **100**, 233 (2004).